

物理学专业本科生在攻读博士期间发表的代表性论文列表

杜增义(1/11) 2008 级	Sign reversal of the order parameter in $(\text{Li}_{1-x}\text{Fex})\text{OHFe}_{1-y}\text{ZnySe}$	Nature Physics 14, 134-139 , 2018
杜增义(1/9) 2008 级	Scrutinizing the double superconducting gaps and strong coupling pairing in $(\text{Li}_{1-x}\text{Fex})\text{OHFeSe}$	Nature Communications 7, 10565, 2016
马桢(1/22) 2011 级	Spin-Glass Ground State in a Triangular-Lattice Compound YbZnGaO_4	Physical review letters 120, 087201, 2018

物理学专业本科生在校期间发表代表性论文列表

作者(X/N)	论文题目	发表期刊、卷页、时间
朱振南(2/7) 王萌萌(3/7)	Interband Optical Absorption in Wurtzite $\text{Mg}_x\text{Zn}_{1-x}\text{O}/\text{ZnO}/\text{Mg}_y\text{Zn}_{1-y}\text{O}$ Asymmetric Quantum Wells	Superlattices and Microstructures, 102, 391-398 ,2017
刘文昊(1/3)	Intersubband optical absorption between multi-levels of electrons in InGaN/GaN spherical core-shell quantum dots	Superlattices and Microstructures, 102, 373-381, 2017
刘文昊(1/3)	Electron mobility limited by optical phonons in wurtzite InGaN/GaN core-shell nanowires	Journal of Applied Physics,122(11) 115104, 2017
李婧(1/5) 关剑宇(2/5)	Effects of ternary mixed crystal and size on optical phonons in wurtzite nitride core-shell nanowires	Journal of Applied Physics 115 (15) :154305, 2014
刘文昊(1/7) 杨露(4/7)	Effects of ternary mixed crystal and size on intersubband optical absorption in wurtzite InGaN/GaN core-shell nanowires	Superlattices and Microstructures, 83, 521-529 ,2015
邢文字(2/6)	Effect of Ho and Mn co-doping on structural, ferroelectric and ferromagnetic properties of BiFeO_3	Thin Solid Films 584, 103,2015

作者(X/N)	论文题目	发表期刊、卷页、时间
	thin films	
董小花 (4/6)	Influence of global and local distortion on magnetic properties of cubic $0.6\text{Ba}0.4-x\text{Ca}x\text{CoO}_3$	Journal of magnetism and magnetic materials 396(2015) 242~246
邢文字(1/6) 马怡妮娜(2/6) 马祯(3/6)	Improved ferroelectric and leakage current properties of Er doped BiFeO_3 thin films derived from the structural transformation	Smart Materials and Structures 2014 , 23 (8) :085030
马祯(2/7) 邢文字(3/7) 马怡妮娜(4/7)	Enhanced ferromagnetism of cluster-assembled BiFeO_3 nanostructured films	Thin solid films 2014 , 570 :351-355
李美玲(3/3)	Dielectric properties and energy-storage performance of $(\text{Na}_{0.5}\text{Bi}_{0.5})\text{TiO}_3$ thick films	Journal of Alloys and Compounds, 601, 112-115, 2014
聂成宏(5/6)	Improved ferroelectric and fatigue properties in Zr doped $\text{Bi}_4\text{Ti}_3\text{O}_{12}$ thin films	Materials Letters 136, 11(2014)
宗易昕 (2/5) 马健 (3/5) 李冬雪 (4/5)	体横光学声子双模性对纤锌矿 $\text{Al}_x\text{Ga}_{1-x}\text{N}$ 量子阱中光学声子的影响	中国科学 .G 辑 , 44(2), 150-161,2014
杨明 (1/3)	Spin-polarized transport through $\text{ZnMnSe}/\text{ZnSe}/\text{ZnBeSe}$ heterostructures	Journal of Applied Physics 110, 093717,2011
袁明虎(1/2)	Quasi-Classical Trajectory Stereodynamics Study of the $\text{Li}+\text{HF}(v=0, j=0) \rightarrow \text{LiF} + \text{H}$ Reaction	International Journal of Quantum Chemistry, 110, 1842-1847, 2010
袁明虎(1/2)	Application of the sixth-order symplectic integration to the chemical stereodynamics for the reactions $\text{Li}+\text{H}(\text{D})\text{F}(v=0, j=0)\rightarrow\text{LiF}+\text{H}(\text{D})$	Journal of Molecular Structure-Theochem 916, 23-27, 2009

ARTICLE

Received 7 Sep 2015 | Accepted 26 Dec 2015 | Published 29 Jan 2016

DOI: 10.1038/ncomms10565

OPEN

Scrutinizing the double superconducting gaps and strong coupling pairing in $(\text{Li}_{1-x}\text{Fe}_x)\text{OHFeSe}$

Zengyi Du^{1,*}, Xiong Yang^{1,*}, Hai Lin^{1,*}, Delong Fang¹, Guan Du¹, Jie Xing¹, Huan Yang¹, Xiyu Zhu¹ & Hai-Hu Wen¹

In the field of iron-based superconductors, one of the frontier studies is about the pairing mechanism. The recently discovered $(\text{Li}_{1-x}\text{Fe}_x)\text{OHFeSe}$ superconductor with the transition temperature of about 40 K provides a good platform to check the origin of double superconducting gaps and high transition temperature in the monolayer FeSe thin film. Here we report a scanning tunnelling spectroscopy study on the $(\text{Li}_{1-x}\text{Fe}_x)\text{OHFeSe}$ single crystals. The tunnelling spectrum mimics that of the monolayer FeSe thin film and shows double gaps at about 14.3 and 8.6 meV. Further analysis based on the quasiparticle interference allows us to rule out the *d*-wave gap, and for the first time assign the larger (smaller) gap to the outer (inner) Fermi pockets (after folding) associating with the d_{xy} (d_{xz}/d_{yz}) orbitals, respectively. The gap ratio amounts to 8.7, which demonstrates the strong coupling mechanism in the present superconducting system.

¹Center for Superconducting Physics and Materials, National Laboratory of Solid State Microstructures and Department of Physics, Collaborative Innovation Center for Advanced Microstructures, Nanjing University, Nanjing 210093, China. * These authors contributed equally to this work. Correspondence and requests for materials should be addressed to H.Y. (email: huanyang@nju.edu.cn) or to H.-H.W. (email: hhwen@nju.edu.cn).

Sign reversal of the order parameter in $(\text{Li}_{1-x}\text{Fe}_x)\text{OHFe}_{1-y}\text{Zn}_y\text{Se}$

Zengyi Du^{1†}, Xiong Yang^{1†}, Dustin Altenfeld^{2†}, Qiangqiang Gu^{1†}, Huan Yang^{1†}, Ilya Eremin², Peter J. Hirschfeld^{3*}, Igor I. Mazin⁴, Hai Lin¹, Xiyu Zhu¹ and Hai-Hu Wen^{1*}

Iron pnictides are the only known family of unconventional high-temperature superconductors besides cuprates. Until recently, it was widely accepted that superconductivity is driven by spin fluctuations and intimately related to the fermiology, specifically, hole and electron pockets separated by the same wavevector that characterizes the dominant spin fluctuations, and supporting order parameters (OP) of opposite signs^{1,2}. This picture was questioned after the discovery of intercalated or monolayer form of FeSe-based systems without hole pockets, which seemingly undermines the basis for spin-fluctuation theory and the idea of a sign-changing OP^{3–11}. Using the recently proposed phase-sensitive quasiparticle interference technique, here we show that in LiOH-intercalated FeSe compound the OP does change sign, albeit within the electronic pockets. This result unifies the pairing mechanism of iron-based superconductors with or without the hole Fermi pockets and supports the conclusion that spin fluctuations play the key role in electron pairing.

In iron pnictides, it has been widely perceived that superconductivity is driven by spin fluctuations, which supports the sign reversal between order parameters (OP) on the electron and hole pockets^{1,2}. The discovery of superconductivity in intercalated or monolayer FeSe at a critical temperature of the order of 40 K rekindled interest in Fe-based superconductivity and sent many theorists back to the drawing board^{3–11}. Indeed, the simple, transparent and largely accepted idea of spin fluctuations scattering electron pairs between hole and electron pockets was shaken by the absence of hole pockets in $\text{K}_x\text{Fe}_{2-y}\text{Se}_2$. The fact that the superconducting phase was formed by filamentary inclusions in a strongly magnetic matrix¹² spoke against a conventional single-sign s -wave (s^{++}) pairing¹³, and model calculations based on the spin-fluctuation scenario predicted a d -wave state^{14,15}, which, by symmetry, would have generated gap nodes¹⁶. On the other hand, later photoemission experiments indicated a nodeless superconducting state^{17,18}. After other materials with similar properties were discovered, including $(\text{Li}_{1-x}\text{Fe}_x)\text{OHFeSe}$, which could be synthesized in a single-phase form^{6,7}, as well as FeSe monolayers⁸, it became increasingly clear that superconductivity at ~ 40 K and higher is possible without hole pockets.

We do not discuss here possible mechanisms for this superconductivity, nor even whether it may or may not be similar to the superconductivity in Fe-pnictides. Instead, we will concentrate on a phenomenological question of utmost importance: is superconductivity in FeSe derivatives (assuming they all belong to the same

class) of a constant OP sign, or does it have a sign-changing OP? The most natural superconductivity of the latter sort is of x^2-y^2 type (where x and y are the directions of the Fe–Fe bonds). As discussed in refs 5,16, crystallographic symmetry-lowering due to the Se positions, and thus doubling of the unit cell, results in this state acquiring gap nodes, although in principle the nodal area may be very small. Moreover, for $\text{K}_x\text{Fe}_{2-y}\text{Se}_2$, which exhibits another electron pocket at the zone centre, this should also lead to nodal lines on this pocket, with a typical cosinusoidal angular dependence of the gap. Neither of these effects has been observed¹⁷. The other type of (truly gapless) sign-changing superconductivity was suggested in ref. 16 and a detailed theory developed by Khodas and Chubukov¹⁹. They observed that upon accounting for the spin–orbit interaction, the folded electron ellipses anti-cross and form two concentric pockets, of which the inner one is mostly of d_{xz}/d_{yz} , and the outer one of d_{xy} orbital character. This ‘bonding–antibonding’ scenario⁵ postulates that the OP on the inner barrel has one sign, and on the outer barrel the other. The goal of this paper is not to distinguish between the $d_{x^2-y^2}$ and s^\pm symmetries, but to eliminate another popular hypothesis, namely that all electron pockets have the same sign of the OP²⁰. We emphasize that this question has a principal conceptual importance; it has been widely argued that no high-temperature superconductivity is possible at all, unless the order parameter averages to (nearly) zero over all Fermi surfaces (thus eliminating the effect of the on-site Coulomb repulsion), and it is generally accepted that spin-fluctuation-driven superconductivity necessarily requires a sign-changing order parameter.

Unfortunately, the phase-sensitive probes developed for d -wave cuprates either fail or are more questionable in Fe-based materials. Probes based on Josephson loops with π -contacts, instead of providing a qualitative test, offer only a quantitative probe, since all possible junctions have currents arising from various Fermi surface sheets corresponding to both same-sign and opposite-sign order parameters^{21,22}. Quasiparticle interference (QPI) due to scattering from vortex cores is, in principle, phase-sensitive, but the interpretation requires specific models of the superconducting states^{23,24}. The technique of identifying bound states formed at a non-magnetic impurity by means of scanning tunnelling microscopy (STM) is more promising, and straightforward to measure. However, here the problem is that it is often hard to prove that the investigated impurities are indeed non-magnetic.

In this paper, we shall report, first, an observation of the above-mentioned bound state, which, notwithstanding the reservations above, strongly suggests a sign-changing order parameter. Second,

¹Center for Superconducting Physics and Materials, National Laboratory of Solid State Microstructures and Department of Physics, Collaborative Innovation Center for Advanced Microstructures, Nanjing University, Nanjing 210093, China. ²Institut für Theoretische Physik III, Ruhr-Universität Bochum, D-44801 Bochum, Germany. ³Department of Physics, University of Florida, Gainesville, Florida 32611, USA. ⁴Code 6393, Naval Research Laboratory, Washington DC 20375, USA. [†]These authors contributed equally to this work. *e-mail: pjh@phys.ufl.edu; hwwen@nju.edu.cn

Spin-Glass Ground State in a Triangular-Lattice Compound YbZnGaO_4

Zhen Ma,¹ Jinghui Wang,¹ Zhao-Yang Dong,¹ Jun Zhang,² Shichao Li,¹ Shu-Han Zheng,¹ Yunjie Yu,² Wei Wang,¹ Liqiang Che,³ Kejing Ran,¹ Song Bao,¹ Zhengwei Cai,¹ P. Čermák,⁴ A. Schneidewind,⁴ S. Yano,⁵ J. S. Gardner,^{5,6} Xin Lu,^{3,7} Shun-Li Yu,^{1,7,*} Jun-Ming Liu,^{1,7} Shiyao Li,^{2,7,†} Jian-Xin Li,^{1,7,‡} and Jinsheng Wen^{1,7,§}

¹National Laboratory of Solid State Microstructures and Department of Physics, Nanjing University, Nanjing 210093, China

²State Key Laboratory of Surface Physics, Department of Physics, and Laboratory of Advanced Materials, Fudan University, Shanghai 200433, China


³Center for Correlated Matter and Department of Physics, Zhejiang University, Hangzhou 310058, China

⁴Jülich Centre for Neutron Science (JCNS) at Heinz Maier-Leibnitz Zentrum (MLZ), Forschungszentrum Jülich GmbH, Lichtenbergstr. 1, 85748 Garching, Germany

⁵National Synchrotron Radiation Research Center, Hsinchu 30077, Taiwan

⁶Center for Condensed Matter Sciences, National Taiwan University, Taipei 10617, Taiwan

⁷Collaborative Innovation Center of Advanced Microstructures, Nanjing University, Nanjing 210093, China

 (Received 30 November 2017; revised manuscript received 12 January 2018; published 22 February 2018)

We report on comprehensive results identifying the ground state of a triangular-lattice structured YbZnGaO_4 as a spin glass, including no long-range magnetic order, prominent broad excitation continua, and the absence of magnetic thermal conductivity. More crucially, from the ultralow-temperature ac susceptibility measurements, we unambiguously observe frequency-dependent peaks around 0.1 K, indicating the spin-glass ground state. We suggest this conclusion holds also for its sister compound YbMgGaO_4 , which is confirmed by the observation of spin freezing at low temperatures. We consider disorder and frustration to be the main driving force for the spin-glass phase.

DOI: [10.1103/PhysRevLett.120.087201](https://doi.org/10.1103/PhysRevLett.120.087201)

Quantum spin liquids (QSLs) represent a novel state of matter in which spins are highly entangled, but neither order nor freeze at low temperatures [1,2]. There is accumulating experimental evidence suggesting that such a state is realized in YbMgGaO_4 [3–11]. The magnetic specific heat C_m is proportional to T^α with $\alpha \approx 2/3$ [3,5,12]. It has a negative Curie-Weiss temperature of $\Theta \sim -4$ K [3,4] but does not show a long-range magnetic order at low temperatures [5,6]. Moreover, diffusive continuous magnetic excitations have been observed by inelastic neutron scattering (INS) measurements [5,6], which are interpreted as resulting from the fractional spin excitations of a QSL [13,14]. However, there are also reports challenging this idea: (i) the thermal conductivity κ study in Ref. [12] reveals no contributions to κ from magnetic excitations despite the large magnetic specific heat at low temperatures, casting doubts on the existence of itinerant quasiparticles expected for a QSL [15]; (ii) since Mg^{2+} and Ga^{3+} in the nonmagnetic layers are randomly distributed [3,4,16], the disorder effect, which is detrimental to the QSL phase for this compound [17], can be significant [5,8].

In this Letter, we report comprehensive measurements on a closely related system, YbZnGaO_4 . We show that the most natural conclusion that is consistent with the micro- and macroscopic data presented here is that the system is a spin glass. We suggest this conclusion to be also true for YbMgGaO_4 , further supported by the observation of spin

freezing at low temperatures. We believe disorder [5,8,11,16,17] and frustration [4,5,11,18–22] to be largely responsible for this phase.

High-quality single crystals of YbZnGaO_4 were grown by the floating-zone technique, overcoming the problem caused by the volatile nature of ZnO [3,23]. The dc and ac magnetic susceptibility and specific heat were measured in a Quantum Design physical property measurement system (see the Supplemental Material [24] for details). INS experiments on the single crystals were carried out on PANDA located at MLZ at Garching, Germany [27]. In the measurements, the 11 coaligned single crystals weighed 1.2 g in total with a sample mosaic of 0.98° and were mounted in the $(H, K, 0)$ plane. INS experiments on the 14-g powder sample were carried out on SIKA located at ANSTO at Lucas Heights, Australia. The wave vector \mathbf{Q} was expressed as the (H, K, L) reciprocal lattice unit (r.l.u.) of $(a^*, b^*, c^*) = (4\pi/\sqrt{3}a, 4\pi/\sqrt{3}b, 2\pi/c)$ with $a = b = 3.414(2)$ Å and $c = 25.140(2)$ Å.

YbZnGaO_4 is isostructural to YbMgGaO_4 , both of which have the YbFe_2O_4 -type structure (space group $R\bar{3}m$, No. 166) [23,28,29]. Schematics of the crystal structure and the two-dimensional triangular lattice of Yb^{3+} are illustrated in Figs. 1(a) and 1(b), respectively. The magnetic ground state of Yb^{3+} ions is a spin-1/2 Kramers doublet [see Fig. 1(d) or Refs. [3,5,8]]. In YbZnGaO_4 , the dc magnetic susceptibility of the effective spin follows the Curie-Weiss



Interband optical absorption in wurtzite $\text{Mg}_x\text{Zn}_{1-x}\text{O}/\text{ZnO}/\text{Mg}_y\text{Zn}_{1-y}\text{O}$ asymmetric quantum wells



Z. Gu, Z.N. Zhu, M.M. Wang, Y.Q. Wang, M.S. Wang, Y. Qu, S.L. Ban*

School of Physical Science and Technology, Inner Mongolia University, Hohhot 010021, People's Republic of China

ARTICLE INFO

Article history:

Received 17 October 2016

Received in revised form 19 October 2016

Accepted 19 October 2016

Available online 31 December 2016

Keywords:

Asymmetric

ZnO/MgZnO quantum well

Electronic interband optical absorption

ABSTRACT

Based on Fermi golden rule, the optical absorption induced by interband transition of electrons and holes in wurtzite $\text{Mg}_x\text{Zn}_{1-x}\text{O}/\text{ZnO}/\text{Mg}_y\text{Zn}_{1-y}\text{O}$ asymmetric quantum wells at room temperature has been discussed. The built-in electric field (BEF) and Poisson potential are considered to calculate the eigenstates and eigenenergies of electrons and holes. The interband optical absorption coefficients (IOACs) influenced by ternary mixed crystal and size effects as functions of incident photon wavelengths are presented. The results indicate that increasing Mg component in left barrier can enhance the BEF to enforce electrons (holes) close to the left (right) interface, so as to reduce the overlapping of their wave functions. Thus the IOAC peak decreases rapidly and presents a blue shift with the increment of Mg component x . Furthermore, the size effect on IOACs is also discussed. The absorption peak is more sensitive to the change of the well width than the left barrier size. The absorption peak reduces sharply and shows a red shift with the increase of the well width. Our results could provide guidance on experiments and device fabrication.

© 2016 Elsevier Ltd. All rights reserved.

1. Introduction

As a representative of II–VI semiconductors, ZnO has attracted much attention due to its wide band gap (3.37 eV) and high exciton binding energy (60 meV) [1,2]. Ternary mixed crystal (TMC) MgZnO has excellent optical properties for its adjustable bandgap versus Mg component [3–5]. Quantum wells (QWs) composed of wurtzite ZnO and MgZnO semiconductors give a good application prospect in the field of ultraviolet electro- and opto-electronic devices, especially for creating UV lasers, photodetectors and all-optical switches [6,7].

In 2002, Zamfirescu et al. [8] predicted ZnO-based microcavity structure to be the most adaptable structure for room temperature polarization laser and it was observed in 2014 [9]. In 2012, photoluminescence spectra were measured as functions of well width in $\text{ZnO}/\text{Mg}_{0.1}\text{Zn}_{0.9}\text{O}$ single QWs with graded thickness [10]. Zhu et al. discussed the intersubband absorption in ZnO/MgZnO QW and effectively control the quantum confinement Stark effect (QCSE) with an external electric field [11]. Their results showed that due to the QCSE the emission band shifts to higher energy with decreasing well width. The QCSE is mainly caused by the built-in electric field (BEF) produced by the spontaneous polarization and the strain-induced piezoelectric polarization [10]. In other works, the linear and nonlinear optical absorptions have been discussed in Ternary/Binary/Ternary (TBT) QWs and quantum dots. The results show that the interband optical absorption coefficients (IOACs) are strongly affected by the component of TMC [12–14], magnetic fields [15], and well widths [14]. In these studies,

* Corresponding author.

E-mail address: siban@imu.edu.cn (S.L. Ban).



Intersubband optical absorption between multi energy levels of electrons in InGaN/GaN spherical core-shell quantum dots



W.H. Liu, Y. Qu*, S.L. Ban

School of Physical Science and Technology, Inner Mongolia University, Key Laboratory of Semiconductor Photovoltaic Technology at Universities of Inner Mongolia Autonomous Region, Hohhot, 010021, PR China

ARTICLE INFO

Article history:

Received 28 July 2016

Accepted 7 August 2016

Available online 31 December 2016

Keywords:

Intersubband optical absorption

Refractive index change

CSQD

Built in electric field

Ternary mixed crystal effect

Size effect

ABSTRACT

The intersubband optical absorption between multi energy levels of electrons in $\text{In}_x\text{Ga}_{1-x}\text{N}/\text{GaN}$ spherical core-shell quantum dots (CSQDs) and ternary mixed crystal and size effects have been investigated by using the principle of density matrix. Electronic eigenstates under the effect of built-in electric field (BEF) have been calculated by a finite element method. The results show that optical absorption between intersubbands with main quantum numbers $n = 1$ and $n = 2$ are as important as that between ones with $n = 1$ and different angular quantum numbers when the BEF is taken into account. In consideration of BEF, the saturation of total optical absorption coefficients (ACs) and secondary peaks of refractive index changes (RICs) appear when incident light intensity I surpasses a certain value. For a given I , the maximum ACs and zero RICs positions in $\text{In}_x\text{Ga}_{1-x}\text{N}/\text{GaN}$ CSQDs with a fixed shell size have a blue-shift when x increases or the core $\text{In}_x\text{Ga}_{1-x}\text{N}$ radius R_1 decreases from 5 nm. However, when $R_1 > 5$ nm, ACs and RICs tend to be stable. The results indicate that effective adjustment of ACs and RICs in CSQDs with BEFs by size is in a limited scale range. The saturation of ACs or secondary peaks of RICs appear more likely in CSQDs with smaller x or larger R_1 . These results are expected to be helpful both in the further theoretical and experimental study on optic devices consisting of CSQDs.

© 2017 Elsevier Ltd. All rights reserved.

1. Introduction

Quasi zero-dimensional quantum dots (QDs), namely artificial atoms have exhibited unique quantum size effects on properties such as atom-like energy levels, tunable bandgaps, etc. [1,2] The improvement in the fabrication of core-shell quantum dots (CSQDs), in which the confinement of carriers along all three directions is enhanced, can be realized and applied to many opto-electronic devices [3,4]. Covering the whole solar spectral region and ranging from the near infrared at $1.9 \mu\text{m}$ (0.64 eV for InN) to the ultraviolet at $0.36 \mu\text{m}$ (3.4 eV for GaN) or $0.2 \mu\text{m}$ (6.2 eV for AlN), wurtzite III-nitride QD systems are important promising materials for light harvesting and emission devices [5]. So far, InGaN/GaN CSQDs have exhibited great perspective in the field of single-photon emitting devices [6], light-emitting diodes [7] or lasers [8] and solar cells [5,9], etc.

Optical absorption coefficients (ACs) and refractive index changes (RICs) are important physical parameters characterizing the sensitive spectral range of opto-electronic devices. According to the selection rules, the optical absorption between permitted intersubbands is an accompanying process in opto-electronic devices. Many effects have been devoted to explore

* Corresponding author.

E-mail address: quyuan@imu.edu.cn (Y. Qu).

Electron mobility limited by optical phonons in wurtzite InGaN/GaN core-shell nanowires

W. H. Liu,¹ Y. Qu,^{1,2,a)} and S. L. Ban^{1,2}

¹School of Physical Science and Technology, Inner Mongolia University, Hohhot 010021, People's Republic of China

²Key Laboratory of Semiconductor Photovoltaic Technology at Universities of Inner Mongolia Autonomous Region, Hohhot 010021, People's Republic of China

(Received 22 March 2017; accepted 4 September 2017; published online 19 September 2017)

Based on the force-balance and energy-balance equations, the optical phonon-limited electron mobility in $\text{In}_x\text{Ga}_{1-x}\text{N}/\text{GaN}$ core-shell nanowires (CSNWs) is discussed. It is found that the electrons tend to distribute in the core of the CSNWs due to the strong quantum confinement. Thus, the scattering from first kind of the quasi-confined optical (CO) phonons is more important than that from the interface (IF) and propagating (PR) optical phonons. Ternary mixed crystal and size effects on the electron mobility are also investigated. The results show that the PR phonons exist while the IF phonons disappear when the indium composition $x < 0.047$, and vice versa. Accordingly, the total electron mobility μ first increases and then decreases with indium composition x , and reaches a peak value of approximately $3700 \text{ cm}^2/(\text{V}\cdot\text{s})$ when $x = 0.047$. The results also show that the mobility μ increases as increasing the core radius of CSNWs due to the weakened interaction between the electrons and CO phonons. The total electron mobility limited by the optical phonons exhibits an obvious enhancement as decreasing temperature or increasing line electron density. Our theoretical results are expected to be helpful to develop electronic devices based on CSNWs. *Published by AIP Publishing.* [<http://dx.doi.org/10.1063/1.5003261>]

I. INTRODUCTION

GaN with high thermal stability and a high breakdown electric field has been widely used in planar high electron mobility transistors (HEMTs). The field-effect transistors (FETs) based on nanowires (NWs) are promising candidates beyond the limitations of planar transistor technology for device scaling.¹ The GaN and its related materials can be well fabricated with perfect crystal quality, making them attractive for NW-based FETs. Gačević *et al.* recently demonstrated a top-gate GaN nanowire metal-semiconductor FET with improved channel electrostatic control.¹ On the other hand, the sensors fabricated based on GaN-NWs also have an excellent performance in Situ Label-Free DNA detections.² The electron mobility is one of the most important fundamental parameters in these electronic devices. Several approaches have been proposed to enhance the electron mobility in NWs, including the utilization of core-shell nanowires (CSNWs),^{3–7} adjustment of composition,^{8,9} and optimization of size.^{10–13} Experiments have demonstrated that the electron mobility could be enhanced to a value comparable to that in high quality undoped bulk GaAs by using CSNW structures, arising from the separation of carriers from the charged and rough surface.³ In GaAs/AlGaAs CSNWs, the Al content can lead to different phonon modes and their intensities⁸ and therefore strongly affects the electron mobility.⁹ The electron mobility in InAs/InAlAs CSNWs showed a monotonic enhancement with increasing core diameters, and an obvious decrease with increasing temperature.⁵ The current-voltage behavior

of fabricated InGaAs NWs has also confirmed the degradation of electron mobility induced by aggressive scaling of the nanowire diameters.¹³

The InGaN in group III-nitride is an ideal candidate in high-speed electronic devices. In planar InGaN/GaN HEMTs, the electron mobility is approximately $2200 \text{ cm}^2/(\text{V}\cdot\text{s})$ in InGaN layer, which is much higher than that in the GaN layer at room temperature.¹⁴ A theoretical analysis using an ensemble Monte Carlo method also revealed that the electron mobility in two dimensional InGaN/GaN systems is higher than that in three dimensional bulk III nitride such as InN, GaN, and AlN.¹⁵ Therefore, the InGaN/GaN CSNWs are expected structures to enhance the quantum confinement of electrons and consequently achieve much higher electron mobility.^{14,15} Nevertheless, the electron mobility in single GaN NWs was reported only approximately $800 \text{ cm}^2/(\text{V}\cdot\text{s})$.¹⁶ Mechanisms of phonons, surface roughness, and remote Coulomb scattering have been discussed to analyze the electron mobility in group III-arsenide NWs.^{17,18} The electron mobility in semiconductor/insulator CSNWs has been calculated using Kubo-Greenwood considering the above mechanisms.^{17–19} It is found that, the scattering from the optical phonons is another important mechanism limiting the electron mobility in InAs NWs besides from the surface roughness.¹⁷ The phonon limitations on the electron mobility have also been investigated in cylindrical Si free standing NWs²⁰ and Si/SiO₂ CSNWs.²¹ At room temperature, the optical phonons become more important than the acoustic ones in affecting electron mobility.¹⁷ However, as far as we know, there is few work focusing on the optical phonons contributions to

^{a)} Author to whom correspondence should be addressed: quyuan@imu.edu.cn

Effects of ternary mixed crystal and size on optical phonons in wurtzite nitride core-shell nanowires

J. Li, J. Y. Guan, S. F. Zhang, S. L. Ban, and Y. Qu^{a)}

School of Physical Science and Technology, Inner Mongolia University, Hohhot 010021, People's Republic of China

(Received 7 March 2014; accepted 4 April 2014; published online 17 April 2014)

Within the framework of dielectric continuum and Loudon's uniaxial crystal models, existence conditions dependent on components and frequencies for optical phonons in wurtzite nitride core-shell nanowires (CSNWs) are discussed to obtain dispersion relations and electrostatic potentials of optical phonons in $\text{In}_x\text{Ga}_{1-x}\text{N}/\text{GaN}$ CSNWs. The results show that there may be four types of optical phonons in $\text{In}_x\text{Ga}_{1-x}\text{N}/\text{GaN}$ CSNWs for a given ternary mixed crystal (TMC) component due to the phonon dispersion anisotropy. This property is analogous to wurtzite planar heterojunctions. Among the optical phonons, there are two types of quasi-confined optical (QCO) phonons (named, respectively, as QCO-A and QCO-B), one type of interface (IF) phonons and propagating (PR) phonons existing in certain component and frequency domains while the dispersion relations and electrostatic potentials of same type of optical phonons vary with components. Furthermore, the size effect on optical phonons in CSNWs is also discussed. The dispersion relations of IF and QCO-A are independent of the boundary location of CSNWs. Meanwhile, dispersion relations and electrostatic potentials of QCO-B and PR phonons vary obviously with size, especially, when the ratio of a core radius to a shell radius is small, and dispersion relation curves of PR phonons appear to be close to each other, whereas, this phenomenon disappears when the ratio becomes large. Based on our conclusions, one can further discuss photoelectric properties in nitride CSNWs consisting of TMCs associated with optical phonons. © 2014 AIP Publishing LLC. [<http://dx.doi.org/10.1063/1.4871544>]

I. INTRODUCTION

Semiconductor radial nanowire (NW) heterostructures open up a substantial opportunity for novel nanoscale photonic and electric devices,^{1,2} such as field effect transistor (FET)³ and light-emitting diodes (LED).⁴ Optical phonons and their interaction with electron have an important influence on optoelectronic properties in low-dimensional quantum systems.⁵⁻⁹ It is known that scattering by optical phonons is one of important scattering mechanisms for electron mobility.⁵ Especially, it plays a main role at room temperature.^{6,7} Luminescence of LED relies on transportation of majority carriers from burning zone to luminous zone through interfaces of heterostructures to create photons by recombination of electrons and holes.⁴ Efficiency of carrier injection in a multi-interface system will be unavoidably lowered by scattering from interface (IF) optical phonons due to the existence of interfaces. Besides, the impurity binding energy in a cylindrical nanowire is found to increase greatly as decreasing the radius of a quantum well wire and can be strongly modified by electron-optical phonon interaction, especially by the interaction with electron-IF optical phonons.⁸ Negative differential resistance in core-shell nanowire heterojunction diodes can also be explained by phonon-assisted interband tunneling mechanism.⁹

Wurtzite GaN and its ternary mixed crystal (TMC), such as $\text{In}_x\text{Ga}_{1-x}\text{N}$ and $\text{Al}_x\text{Ga}_{1-x}\text{N}$ have been applied extensively to the planar optoelectronic device for their excellent properties.¹⁰ Through controlled growth and organization, there is a growing interest in the development of nanoscale devices using wurtzite nitride and relative TMC as important candidates for core-shell nanowires (CSNWs) based devices.^{3,4} The performance of devices can be modified directly by adjusting the size and component of TMC contained in a planar system,⁷ and one may reasonably expect that the adjustment of TMC and size can also be an effective way to improve performance in CSNWs based devices. The property of optical phonons and their interaction with electrons in CSNWs are more complicated due to the curved interfaces and TMC effect. Therefore, a detailed theoretical investigation of TMC and size effects on optical phonons in CSNWs is helpful to promote the development both in theory and in experiment.

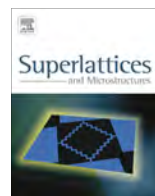
The theory of confined, propagating (PR), half-space (HS), and IF optical phonon modes in wurtzite planar heterostructures has been first formulated by Dutta *et al.*¹¹⁻¹³ Recently, Zhang *et al.* have conducted a series of research works on optical phonons in CSNWs by employing the dielectric continuum and Loudon's uniaxial crystal models.¹⁴⁻¹⁷ The IF optical phonons and a Fröhlich-type electron-phonon interaction Hamiltonian in wurtzite GaN/AlN CSNWs have been derived and studied.¹⁴ Dispersion relations of quasi-confined (QCO), half-space, propagating optical phonons and the electron-phonon

^{a)}Author to whom correspondence should be addressed. Electronic mail: quyuan@imu.edu.cn. Tel.: +86 471 4992914.



Contents lists available at ScienceDirect

Superlattices and Microstructures

journal homepage: www.elsevier.com/locate/superlattices

Effects of ternary mixed crystal and size on intersubband optical absorption in wurtzite InGaN/GaN core-shell nanowires



W.H. Liu, S. Yang, H.M. Feng, L. Yang, Y. Qu*, S.L. Ban

School of Physical Science and Technology, Inner Mongolia University, Key Laboratory of Semiconductor Photovoltaic Technology at Universities of Inner Mongolia Autonomous Region, Hohhot 010021, PR China

ARTICLE INFO

Article history:

Received 17 March 2015

Accepted 19 March 2015

Available online 27 March 2015

Keywords:

Intersubband optical absorption

CSNW

Ternary mixed crystal effect

Size effect

ABSTRACT

Based on the density matrix approach, the effects of ternary mixed crystal and size on intersubband optical absorption coefficients in $\text{In}_x\text{Ga}_{1-x}\text{N}/\text{GaN}$ core-shell nanowires (CSNWs) are investigated. The results show that the optical absorption can be modulated by In component x and the size of CSNWs, since the variation of electron states in these systems. It is found that photonic frequencies of resonant absorption and the absorption coefficient increase obviously when x increases or the radius of InGaN core reduces, while the half-width of the coefficient decreases as its peak becomes higher and sharper. A saturation phenomenon of optical absorption is also found when the incident light intensity exceeds a certain value. The theoretical results are expected to be helpful to develop CSNW optic devices.

© 2015 Published by Elsevier Ltd.

1. Introduction

Core-shell nanowires (CSNWs) consisting of semiconductors have indicated great prospects for opto-electronic applications, such as solar cells [1–3], optical cavities [4], antennas [5], lasers [6], and et al., due to their effective optical absorption and related phenomena. Optical absorption enhancement may reduce the cost and improve the efficiency of optic devices [1–6]. Nowadays, many

* Corresponding author. Tel.: +86 471 4992914.

E-mail address: quyuan@imu.edu.cn (Y. Qu).



Effect of Ho and Mn co-doping on structural, ferroelectric and ferromagnetic properties of BiFeO₃ thin films



Qi Yun, Wenyu Xing, Jieyu Chen, Wei Gao, Yulong Bai, Shifeng Zhao*

School of Physical Science and Technology, Inner Mongolia Key Lab of Nanoscience and Nanotechnology, Inner Mongolia University, Hohhot 010021, PR China

ARTICLE INFO

Available online 15 November 2014

Keywords:

Ferroelectric properties
Ferromagnetic properties
Structural transformation
Doping

ABSTRACT

Multiferroic pure, Ho doped, Mn doped, as well as Ho, Mn co-doped BiFeO₃ thin films were prepared using a sol-gel technique. The effect of Ho and Mn co-doping on the structure, ferroelectric and ferromagnetic properties of BiFeO₃ films was studied in detail. It shows that the enhanced ferroelectric polarization and magnetization were obtained after doping Ho and Mn. Such enhanced ferroelectric properties are attributed to ferroelectric distortion derived from the structural transformation and microstructure improvement after doping Ho and Mn. The enhanced ferromagnetic properties are attributed to the uncompensated surface spins and the release of the latent magnetization locked within the cycloid induced by doping Ho and Mn. The present work provides an easy method to enhance the ferroelectric and ferromagnetic properties of BiFeO₃ based magnetoelectric multiferroic films.

© 2014 Elsevier B.V. All rights reserved.

1. Introduction

Magnetoelectric multiferroics, showing simultaneous ferroelectric and ferromagnetic orders, have aroused wide attention in recent years, because they offer a wide range of potential applications in data storage media, spintronics and multi-state memories [1–5]. As one of representative single phase multiferroics, BiFeO₃ (BFO) with rhombohedrally distorted perovskite structure, exhibits simultaneously ferroelectric behavior with high ferroelectric Curie temperature and G-type antiferromagnetic behavior with a relatively high Néel temperature [6]. Those advantages make it very attractive from an application point of view. Although BiFeO₃ materials have these outstanding advantages, it is difficult to gain a large spontaneous polarization and magnetization [7,8], which limits their further applications in magnetoelectric materials. On the one hand, for BFO materials, ferroelectricity originates from the relative displacement of cations resulting from the stereochemical activity of 6 s² lone pair electrons of Bi³⁺ ions [9]. The weak polarization of BFO thin films is attributed to the defects such impurity phases and oxygen vacancies. And the formation of oxygen vacancies induces impurity energy level in the band gap and increases the free carrier density by hopping of electrons to these defect levels [10]. On the other hand, the weak magnetization is attributed to the superimposition of a spiral spin structure on BFO antiferromagnetic order. In this spiral spin structure, the antiferromagnetic axis rotates through the crystal with an incommensurate long wavelength period of 62 nm [11], which cancels the macroscopic magnetization and also inhibits the observation of the linear magnetoelectric effect in bulk BiFeO₃. Much work has been carried out to address these

difficulties, including adding small amount of substitution [12,13], preparing nano-size materials [14–16] or epitaxial films [17]. Among these methods, rare earth iron doped at Bi site and transitional metal doped at Fe site are thought to be an effective way to improve the ferroelectric and ferromagnetic properties at room temperature. Therefore, it is widely expected that the strategies based on nanotechnology and aliovalent ion doping will have a great impact on their magnetic, electric and magnetoelectric properties as a result of the suppression of the helical order and quantum confinement effect [18,19]. Based on those above, in this study, pure BiFeO₃, Bi_{0.9}Ho_{0.1}FeO₃ (BHFO), BiFe_{0.9}Mn_{0.1}O₃ (BFMO), and Bi_{0.9}Ho_{0.1}Fe_{0.9}Mn_{0.1}O₃ (BHFMO) thin films were prepared on Pt(100)/Ti/SiO₂/Si substrates via a solution–gelation method. The crystal structures, and microstructural, ferroelectric and ferromagnetic properties were investigated. It shows that the obviously improved ferroelectric and ferromagnetic properties were obtained after doping Ho and Mn. The origins of the improved electric and magnetic properties are discussed in detail.

2. Experiment details

Bi_{1-x}Ho_xFe_{1-y}Mn_yO₃ (x = 0, y = 0; x = 0.1, y = 0; x = 0, y = 0.1; x = 0.1, y = 0.1), namely, BiFeO₃ (BFO), Bi_{0.9}Mn_{0.1}FeO₃ (BMFO), BiFe_{0.9}Mn_{0.1}O₃ (BFMO) and Bi_{0.9}Ho_{0.1}Fe_{0.9}Mn_{0.1}O₃ (BHFMO) were synthesized by the solution–gelation method. The raw materials used for the precursor solutions are bismuth nitrate pentahydrate [Bi(NO₃)₃·5H₂O], iron nitrate nonahydrate [Fe(NO₃)₃·9H₂O], holmium nitrate pentahydrate [Ho(NO₃)₃·5H₂O], and manganese acetate tetrahydrate [C₄H₆MnO₄·4H₂O]. Bismuth nitrate pentahydrate and iron nitrate nonahydrate were added to the ethylene glycol solvent in proportions of 1.1:1, with excess 10% Bi for compensating the loss during annealing. Then stir the solution until the solution is clear transparent at room temperature. The preparation methods of BHFO, BFMO and BHFMO

* Corresponding author at: School of Physical Science and Technology, Inner Mongolia University, Hohhot 010021, China. Tel./fax: +86 471 499 3141.
E-mail address: zhshf@imu.edu.cn (S. Zhao).



Influence of global and local distortion on magnetic properties of cubic $\text{La}_{0.6}\text{Ba}_{0.4-x}\text{Ca}_x\text{CoO}_3$



Hong Chang^{a,b,*}, Yu Gao^{a,b}, Qiang Wu^{a,b}, Xiaohua Dong^{a,b}, Yunfei Li^{a,b}, Yanbo Pang^{a,b}

^a School of Physical Science and Technology, Inner Mongolia University, Hohhot 010021, China

^b Inner Mongolia Key Lab of Nanoscience and Nanotechnology, Hohhot 010021, China

ARTICLE INFO

Article history:

Received 20 May 2015

Received in revised form

27 July 2015

Accepted 7 August 2015

Available online 9 August 2015

Keywords:

Ferrimagnetic

LaCoO_3

Global and local distortion

ABSTRACT

The magnetic and structural study of the $\text{La}_{0.6}\text{Ba}_{0.4-x}\text{Ca}_x\text{CoO}_3$ ($x=0.0, 0.1, 0.2, 0.3$, and 0.4) compounds with the lowest global or local distortion are studied. The compounds with $x=0, 0.1, 0.2$ and 0.3 is crystallized in the structure with the space group $Pm-3m$, and that with $x=0.4$ is $Pnma$. A ferromagnetic-like transition is observed and the Curie temperature, ranging from 235 K to 220 K, decreases slightly with the increasing Ca^{2+} content for $x \leq 0.3$, and the transition temperature is as low as 175 K with $x=0.4$. A hump, with the hump temperature slightly increase with the Ca^{2+} content, is observed in the thermal magnetization curves of all of the compounds at the ZFC state, and it is owing to the magnetic frustration because of the coexistence of the FM and the AFM interaction. Above the transition temperature, the magnetic susceptibility versus the temperature is fitted with the ferromagnetic Curie-Weiss law for the compounds with $x \leq 0.3$, and that with $x=0.4$ coincides with the ferrimagnetic Weiss-mean-field model. The absolute values of the exchange constants J_1 in the compounds with $x \leq 0.3$ and those of $J_{\text{Co}^{3+}\text{Co}^{3+}}, J_{\text{Co}^{3+}\text{Co}^{4+}}, J_{\text{Co}^{4+}\text{Co}^{4+}}$ of $\text{La}_{0.6}\text{Ca}_{0.4}\text{CoO}_3$ are deduced from the fitting. The results indicate that (i) the ferromagnetic exchange constants J_1 increases with the Ca^{2+} content $x \leq 0.3$; (ii) the ferromagnetic interaction, $J_{\text{Co}^{3+}\text{Co}^{4+}}$, plays a main role in the magnetic properties of $\text{La}_{0.6}\text{Ca}_{0.4}\text{CoO}_3$; (iii) the antiferromagnetic interactions, $J_{\text{Co}^{3+}\text{Co}^{3+}}, J_{\text{Co}^{4+}\text{Co}^{4+}}$, are not negligible in the compound $x=0.4$. The unsaturated magnetization at 70 kOe and the high coercive field in the hysteretic magnetization curve supports the existence of the antiferromagnetic interaction, and the percentage of the antiferromagnetic domain is calculated.

© 2015 Elsevier B.V. All rights reserved.

1. Introduction

The LaCoO_3 compound is the focus of research, since the Co ions exhibit the spin state transitions and the character of the itinerant carriers [1,2]. The spin configuration of the Co^{3+} ions features as $3d^6$, and it can be at 3 different spin states: a low spin state (LS: $t_{2g}^6 e_g^0$; $S = 0$), an intermediate spin state (IS: $t_{2g}^5 e_g^1$; $S = 1$), and a high spin state (HS: $t_{2g}^4 e_g^2$; $S = 2$). In the ground state, LaCoO_3 is a non-magnetic insulator with the Co^{3+} ions at the LS state, but with increasing the temperature a paramagnetic insulating state develops above about 50 K and around 500 K an insulator to metal transition is observed [3–5]. At $T=0$ K, the spin state is at a LS diamagnetic state with 6 paired t_{2g} electrons and no electrons in the nominally higher energy e_g states. While the temperature drives the electron to transfer from the t_{2g} to the e_g orbitals, the Co ions

* Corresponding author at: School of Physical Science and Technology, Inner Mongolia University, Hohhot 010021, China.

E-mail address: changhong@imu.edu.cn (H. Chang).

develop into the two possible higher spin states. The increase of the temperature excites the spins either to a mixture of the LS state and the HS state, or to a mixture of the LS state and the IS state [5,6]. While the La^{3+} ions are partly substituted by the divalent earth-alkaline elements such as $A=\text{Ca}^{2+}, \text{Sr}^{2+}$, or Ba^{2+} , the charge-carrier doping creates Co^{4+} ions in order to get a valence balance. The Co^{4+} ions featured as $3d^5$ are magnetic in all possible spin states: $t_{2g}^5 e_g^0$, $S = \frac{1}{2}$ (LS); $t_{2g}^4 e_g^1$, $S = \frac{3}{2}$ (IS); $t_{2g}^3 e_g^2$, $S = \frac{5}{2}$ (HS).

The transfer interaction of the e_g -state conduction electron between the neighboring Co sites is a key factor in determining the magnetic and electronic states. It depends on the lattice distortion of the perovskite structure. The lattice distortion is described by the global distortion in terms of the tolerance factor and the local distortion from the different ionic radii at A-site. The global distortion is described by the tolerance factor $t = \frac{(r_A) + (r_O)}{\sqrt{2}((r_{\text{Co}}) + (r_{\text{O}}))}$ and the local distortion is $r_A = (1-x)r_{\text{La}^{3+}} + xr_{\text{M}^{2+}}$, where r_{Co} , r_{O} , r_{La} and r_{M} denote the ionic radii of the Co, the O, the La and the M^{2+} ($\text{Ca}^{2+}, \text{Sr}^{2+}, \text{Ba}^{2+}$, etc.) ions. In the La–Ba–Co–O compounds, the Ba^{2+} ions reduce the global distortion from the ideal perovskite structure. Especially, the

Improved ferroelectric and leakage current properties of Er-doped BiFeO₃ thin films derived from structural transformation

Wenyu Xing^{1,3}, Yinina Ma^{1,3}, Zhen Ma¹, Yulong Bai¹, Jieyu Chen¹ and Shifeng Zhao^{1,2,3}

¹School of Physical Science and Technology, Inner Mongolia University, Hohhot, 010021, People's Republic of China

²Inner Mongolia Key Lab of Nanoscience and Nanotechnology, Inner Mongolia University, Hohhot, 010021, People's Republic of China

E-mail: zhsf@imu.edu.cn

Received 19 May 2014, revised 4 June 2014

Accepted for publication 8 June 2014

Published 8 July 2014

Abstract

Multiferroic pure and Er-doped BiFeO₃ thin films were prepared using a sol–gel technique. The effect of Er-doped concentration on the crystal structure and on the ferroelectric and leakage current properties of BiFeO₃ films were studied in detail. The study showed the enhanced ferroelectric polarization and reduced leakage current density that occurred after doping Er. Such improved ferroelectric and leakage properties are attributed to ferroelectric distortion and to the change of leakage current conduction mechanisms derived from the structural transformation that occurred after doping Er. The rhombohedral structure of pure BiFeO₃ transforms to the coexistence of tetragonal and orthorhombic symmetry structure as Er-doped concentration x increased gradually to 0.15, then to the orthorhombic structure when $x=0.20$. The present work provides an easy method to decrease the leakage current and improve the ferroelectric properties of BiFeO₃ films.

Keywords: ferroelectric properties, leakage current, structural transformation

(Some figures may appear in colour only in the online journal)

1. Introduction

Multiferroics have attracted a great deal of attention due to the simultaneous coexistence of ferromagnetic, ferroelectric, or ferroelastic ordering [1, 2]. Many previous research projects have been focused on the magnetoelectric effect caused by the prospect of controlling polarization by magnetic fields and magnetization by an electric field [3], which opens up an entirely new perspective of magnetic/ferroelectric data storage media, spin-based devices (spintronics), magneto–capacitive devices, magnetic sensors, nonvolatile memory, random access memory, etc [4–8]. The new kinds of micro devices and functionality offered by multiferroics rely entirely on their size-dependent physical and chemical properties, which have aroused extensive research activity in this area. BiFeO₃

is a most promising candidate as a magnetoelectric material due to its above-room-temperature ferroelectric Curie temperature ($T_C \sim 1143$ K) [2] and antiferromagnetic Néel temperature ($T_N \sim 643$ K) [7]. For BiFeO₃ materials with a rhombohedrally distorted perovskite structure belonging to the space group R3c [7], ferroelectricity originates from the relative displacement of cations resulting from the stereochemical activity of 6s² lone pair electrons of Bi³⁺ ions [9]. However, it is difficult to gain a large saturation and remnant polarization in BiFeO₃ materials due to the higher leakage current arising from defects such as impurity phases and oxygen vacancies [10, 11]. Much work has been carried out to address these difficulties, including adding a small amount of substitution or preparing epitaxial films [12–16]. Among these methods, rare-earth iron doped at a Bi site is thought to be an effective way to improve ferroelectric properties at room temperature [17–19]. However, most of these studies

³ These authors contributed equally to this work.



Enhanced ferromagnetism of cluster-assembled BiFeO₃ nanostructured films



Shifeng Zhao^{a,b,*}, Zhen Ma^a, Wenyu Xing^a, Yinina Ma^a, Alima Bai^a, Qi Yun^a, Jieyu Chen^a

^a School of Physical Science and Technology, Inner Mongolia University, Hohhot 010021, People's Republic of China

^b Inner Mongolia Key Lab of Nanoscience and Nanotechnology, Inner Mongolia University, Hohhot 010021, People's Republic of China

ARTICLE INFO

Available online 14 February 2014

Keywords:

Cluster
Enhanced ferromagnetism
Nanostructured films
Multiferroics

ABSTRACT

Cluster-assembled BiFeO₃ nanostructured films were prepared using low-energy cluster beam deposition method with our homemade cluster apparatus. It is shown that the nanostructured films are perovskite structure and assembled uniformly and compactly with monodisperse spherical clusters with average diameter of ~22 nm. The enhanced ferromagnetism is observed for the as-prepared films, which is attributed to the uncompensated surface spins and the release of the latent magnetization locked within the cycloid induced by the size effect of the clusters with the smaller characteristic size than the long-range cycloid order of 62 nm. The present work provides a way on enhancing ferromagnetism of single-phase multiferroics.

© 2014 Elsevier B.V. All rights reserved.

1. Introduction

Recently, there has been increasing interest in multiferroics due to their potential applications in magnetoelectric energy conversion devices [1,2]. Some single-phase materials such as Cr₂O₃, BiFeO₃, YMnO₃, TbMnO₃ and others [3–5] exhibit multiferroic properties. Among those multiferroic materials, BiFeO₃ (BFO) is one of the most outstanding single-phase lead-free multiferroics due to its high ferroelectric Curie ($T_{FE} \sim 1103$ K) and Neel ($T_N \sim 643$ K) temperatures. However, for BFO materials, antiferromagnetism and a superimposed incommensurate cycloid spin structure with a periodicity of 62 nm along the [1 1 0]_h axis cancel the macroscopic magnetization at room temperature, which restricts its applications [6]. Attempts to enhance the ferromagnetism include the preparation of epitaxial BFO films [7] as well as B-site-ion-doped BFO compounds [8–11]. Further, some investigations show that weak ferromagnetism is observed in some limited-dimension materials such as nanowires and nanoparticles due to the partial destruction of the spiral periodicity [12–14], which demonstrates a possible way to enhance ferromagnetism in single-phase multiferroics. Specifically, there have been recent developments concerning the enhancement of ferromagnetism for BFO materials by the nanostructure modulation [14–16] such as controlling the size of the nanoparticles or the thickness of the thin films. Therefore, in this work, we attempt to enhance ferromagnetism of BFO films by preparing the nanostructured films assembled with clusters, which are dimension limited and have smaller characteristic size than the periodicity of 62 nm.

We have developed a low-energy cluster beam deposition (LECBD) technique for effective preparation of well-defined 0-characteristic-dimension nanostructured materials, i.e., the cluster [17,18], which is an ideal building block to assemble the nanostructures. Some cluster-assembled nanostructured films such as metals, simple metallic oxides, alloys and heterostructures have been prepared. Each exhibits particular physical and chemical properties related to the size effect of the nanocluster [17–21]. Using this technique, we have prepared the well-defined BiFeO₃ nanostructured films assembled with 0-characteristic-dimension clusters. As we expected, the ferromagnetism of the as-prepared BiFeO₃ films is enhanced. The origin of such enhanced ferromagnetism for the cluster-assembled BiFeO₃ nanostructured films was analyzed. Further, it suggests that the magnetic properties of the cluster-assembled BiFeO₃ nanostructured films could be controlled by changing the size and the assembling manner of the BiFeO₃ clusters, which makes it an ideal candidate for the coexistence of ferromagnetism and ferroelectricity in the same phase.

2. Experiment details

A magnetron-sputtering-gas-aggregation cluster source was used to produce the cluster beam. A BiFeO₃ plate with diameter of 50 mm and thickness of 3 mm was used as the sputtering target. A direct current pulse power was used as the sputtering power due to the insulating properties of the BiFeO₃ plate target. As the sputtering gas, one stream of argon gas with 99.9% purity was introduced through a ring structure close to the surface of the BiFeO₃ target. Another stream of argon was fed as a buffer gas through a gas inlet near the magnetron discharge head. The cluster condensation and growth region was cooled with liquid nitrogen. A highly oriented cluster beam with a small divergent angle less than one degree was formed by differential pumping

* Corresponding author at: School of Physical Science and Technology, Inner Mongolia University, Hohhot 010021, China. Tel./fax: +86 471 499 3141.
E-mail address: zhshf@imu.edu.cn (S. Zhao).



Dielectric properties and energy-storage performance of $(\text{Na}_{0.5}\text{Bi}_{0.5})\text{TiO}_3$ thick films



Ye Zhao^a, Xihong Hao^{a,*}, Meiling Li^b

^a School of Materials and Metallurgy, Inner Mongolia University of Science and Technology, Baotou 014010, China

^b College of Physics and Technology, Inner Mongolia University, Hohhot 010020, China

ARTICLE INFO

Article history:

Received 13 December 2013

Received in revised form 20 February 2014

Accepted 22 February 2014

Available online 4 March 2014

Keywords:

NBT thick films

Sol–gel

Energy-storage performance

Leakage current

ABSTRACT

Lead-free ferroelectric $\text{Na}_{0.5}\text{Bi}_{0.5}\text{TiO}_3$ (NBT) thick films were successfully fabricated on LaNiO_3/Si (100) substrates by using a polyvinylpyrrolidone (PVP)-modified sol–gel technique. The dielectric properties, energy-storage performance and leakage current characteristics were investigated in detail. At 100 kHz, the capacitance density of the NBT thick films was 295 nF/cm^2 . The maximum recoverable energy-storage density and efficiency of the sample were 12.4 J/cm^3 and 43% at 1200 kV/cm , respectively. A low leakage current density of about $1 \times 10^{-5} \text{ A/cm}^2$ was also obtained at 700 kV/cm at room temperature. These results indicated that the lead-free ferroelectric NBT thick films might be the promising candidates for high energy-storage capacitors application.

© 2014 Elsevier B.V. All rights reserved.

1. Introduction

Energy-storage capacitors play a vital role in pulse power circuits which are utilized to generate large amounts of electrical energy within an extremely short time period. With the developments of the micro-electronics technologies, high energy-storage density capacitors with decreased volume, weight and cost are urgently needed [1–6]. Commonly, the recoverable energy-storage density W could be estimated from the polarization–electric field hysteresis (P – E) loops, which is calculated with the equation as below:

$$W = \int_{P_r}^{P_{max}} E dP, \quad (1)$$

where E is the applied electric field, P is the polarization, P_r is the remnant polarization and P_{max} is the maximum polarization. Considering to Eq. (1), materials with smaller P_r , larger P_{max} and higher breakdown strength (BDS) are more suitable for high energy-storage application. Because of the high maximum polarization and nearly zero remnant polarization, antiferroelectrics (AFE) as high energy-storage materials have been widely studied [7–9].

Up to now, the reported works on energy-storage AFE materials were mainly focused on bulk ceramics and thin films [10,11]. Because of the lower breakdown field, the energy-storage density of the bulk ceramics is usually very small. For example, it was

reported that the maximum recoverable energy-storage density in $0.89(\text{Na}_{0.5}\text{Bi}_{0.5})\text{TiO}_3\text{--}0.06\text{BaTiO}_3\text{--}0.05(\text{K}_{0.5}\text{Na}_{0.5})\text{NbO}_3$ ceramics was only 0.59 J/cm^3 [12]. Although thin films (thickness $< 1 \mu\text{m}$) possess good electric field endurance, their overall stored energy is quite small due to their thickness limitations. Mirshekarloo et al. reported a moderate recoverable energy-storage density of about 11 J/cm^3 in $(\text{Pb}_{0.97}\text{La}_{0.02})(\text{Zr}_{1-x-y}\text{Sn}_x\text{Ti}_y)\text{O}_3$ AFE thin films [7]. Comparatively, thick films (thickness $> 1 \mu\text{m}$) could conquer the shortcomings in bulk ceramics and thin films and be suitable for the application in high energy-storage capacitors. A large recoverable energy-storage density of 56 J/cm^3 was obtained in $(\text{Pb},\text{La})(\text{Zr},\text{Sn},\text{Ti})\text{O}_3$ AFE thick films [13].

Currently, the most studied energy-storage materials are lead-based [14]. Scared by the serious environmental problems as a result of using lead-based materials, the European Union and some other countries have legislated to eliminate the use of lead [15,16]. Therefore, developing lead-free and high energy-storage materials becomes inevitable. Sodium bismuth titanate $(\text{Na}_{0.5}\text{Bi}_{0.5})\text{TiO}_3$ (NBT), discovered by Smolenski et al. in 1961 [17], is a typical perovskite-type ferroelectrics with Na^+ and Bi^{3+} at A site. Pure NBT is ferroelectric (FE) phase, with rhombohedral structure, at room temperature. It was also found that, with the temperature increasing, it experienced a phase transition from FE to AFE at $140 \text{ }^\circ\text{C}$, and then to paraelectric (PE) phase at its Curie temperature (T_c) of about $320 \text{ }^\circ\text{C}$ [18]. Moreover, the critical temperature corresponding to the appearance of AFE phase could be declined by chemical substitution, such as BaTiO_3 and $\text{K}_{0.5}\text{Na}_{0.5}\text{NbO}_3$ [12]. Accordingly, it is believed that NBT-based materials have the

* Corresponding author. Tel.: +86 472 5951572; fax: +86 472 5951571.

E-mail address: xhhao@imust.cn (X. Hao).

Research Article

Improved Ferroelectric and Leakage Properties of Ce Doped in BiFeO₃ Thin Films

Alima Bai, Shifeng Zhao, and Jieyu Chen

School of Physical Science and Technology and Inner Mongolia Key Lab of Nanoscience and Nanotechnology, Inner Mongolia University, Hohhot 010021, China

Correspondence should be addressed to Shifeng Zhao; zhsf@imu.edu.cn

Received 10 May 2014; Accepted 20 May 2014; Published 8 June 2014

Academic Editor: Daniela Predoi

Copyright © 2014 Alima Bai et al. This is an open access article distributed under the Creative Commons Attribution License, which permits unrestricted use, distribution, and reproduction in any medium, provided the original work is properly cited.

Ce doped BiFeO₃ thin films with a perovskite structure were prepared using solution-gelation method. It shows that the ferroelectric properties have been enhanced after doping Ce. The enhanced ferroelectric properties are attributed to the structural transformation and the reduced leakage current after doping rare metal of Ce. It has been found that the phase structures of the films transfer from rhombohedral symmetry structure to the coexistence of the tetragonal and orthorhombic symmetry structure. And Fe²⁺ ions have been reduced, which leads to the decreased leakage for Ce doped BiFeO₃ thin films. The present work can provide an available way to improve the ferroelectric and leakage properties for multiferroic BiFeO₃ based thin films.

1. Introduction

Multiferroic materials exhibit ferroelectric, ferromagnetic, and ferroelasticity properties simultaneously in a certain temperature range. The single phase BiFeO₃ (BFO) materials with perovskite structure have aroused wide concerns due to its high curie temperature (T_N) of 1103 K and Neil temperature (T_C) of 643 K [1], which make it a most promising candidate in ferroelectric memory storage and magnetoelectric devices [2–5]. However, for BiFeO₃ materials with a rhombohedrally distorted perovskite structure belonging to the space group R3c, it is difficult to gain a large saturation and remnant polarization due to the higher leakage current arising from defects such as impurity phases and oxygen vacancies [6, 7]. Several investigations have been carried out to prove that it is an effective approach for rare earth iron doping at Bi site to overcome the technical barrier and improve the ferroelectric and leakage properties of BiFeO₃ materials [8–10]. Evidently, donor and acceptor dopants have contrary effects on modulating the charged defects. Thus, it becomes necessary to further understand how they affect the respective polarity and polarization stability of BiFeO₃ thin films. However, most of these studies were focused on ceramics and bulk materials [11, 12], which are not fit for the rapidly developing micro- and nanoelectromechanical system (MEMS&NEMS).

Therefore, in this work, Ce doped BiFeO₃ thin films were prepared using solution-gelation method as this technique can well control the stoichiometric ratio. Ce will replace Bi of A sites in perovskite structure of ABO₃. The choice of the dopant ion was based on the fact that Ce³⁺ has a more stable electronic configuration than Bi³⁺, which minimizes the leakage current and further improves ferroelectric properties in BiFeO₃ thin films. The origins of the improved ferroelectric and leakage properties are discussed in detail in this paper. The present work can provide an available way to improve the ferroelectric properties for single phase multiferroic BiFeO₃ based thin films.

2. Experiment

The pure and Ce doped BiFeO₃ thin films were prepared using the solution-gelation method. All the reactions were carried out at room temperature under ambient conditions. High-purity bismuth nitrate [Bi(NO₃)₃·5H₂O], ferric nitrate [Fe(NO₃)₃·9H₂O], and cerium nitrate [Ce(NO₃)₃·6H₂O] were obtained from commercial sources (Alfa Aesar); they were dissolved in solvent ethylene glycol monomethyl ether in proper proportions of 0.99:1:0.1 and stirred until the solutions turn into transparent for about three to four hours.



论文

体横光学声子双模性对纤锌矿 $\text{Al}_x\text{Ga}_{1-x}\text{N}$ 量子阱中光学声子的影响

屈媛, 宗易昕, 马健, 李冬雪, 班士良*

内蒙古大学物理科学与技术学院, 呼和浩特 010021

*联系人, E-mail: slban@imu.edu.cn

收稿日期: 2013-04-06; 接受日期: 2013-05-23

国家大学生创新性试验计划项目(编号: 101012608)和国家自然科学基金(批准号: 61274098)资助项目

摘要 本文采用介电连续模型讨论纤锌矿 $\text{Al}_x\text{Ga}_{1-x}\text{N}$ 的体横光学(TO)声子双模性对其量子阱中光学声子的影响. 首先, 给出 $\text{Al}_x\text{Ga}_{1-x}\text{N}$ 中 TO 声子的频率的二次多项式拟合公式, 在组分 $x=0$ 和 $x=1$ 时, 使 TO 声子频率可回归至 GaN 和 AlN 情形. 进而, 分析 $\text{Al}_x\text{Ga}_{1-x}\text{N}$ 含频介电函数随组分的变化. 结果显示 TO 声子频率的单模或双模性将影响单个或两个共振频率下的含频介电函数; 最后, 以 AlN/ $\text{Al}_x\text{Ga}_{1-x}\text{N}$ /AlN 量子阱为例, 计算界面和局域光学声子色散关系和声子静电势的影响. 结果表明, 纤锌矿 $\text{Al}_x\text{Ga}_{1-x}\text{N}$ 的 TO 声子双模性在量子阱光学声子以及相关的理论计算中是不可忽略的.

关键词 纤锌矿, 量子阱, 三元混晶, 色散关系, 声子静电势

PACS: 63.20.Dj, 68.65.Fg, 74.70.Dd

doi: 10.1360/132013-161

1 引言

纤锌矿三元混晶 $\text{Al}_x\text{Ga}_{1-x}\text{N}$ 及其异质结构在发光二极管、高电子迁移率晶体管等光电子器件方面有重要应用, 可通过改变混晶组分在大范围内调节其光电性质, 并可在特定组分下表现优良性能^[1-3]. 纤锌矿氮化物量子阱是一种常见的异质结构, 由于增强对电子的束缚作用而比传统单异质结具有更小的漏电流和更高的击穿电压^[4]等优异特性. Qu 等人^[5]在讨论室温下 InGaN 凹槽层的引入对 AlN/GaN/AlN 量子阱中电子迁移率的作用时, 发现随着 In 组分的改

变使量子阱光学声子的发生模式转变, 进而影响主要决定于光学声子散射作用的电子迁移率.

电子-声子相互作用是影响半导体器件光电性质的重要机制, 例如室温下光学声子散射就对电子迁移率起主要作用^[5,6]. 国外研究者通过拉曼谱分析发现, 纤锌矿 $\text{Al}_x\text{Ga}_{1-x}\text{N}$ 的体纵光学(LO)声子频率表现出单模性, 而体横光学(TO)声子频率则为双模性^[7]. 在理论上, 对三元混晶(TMC)体光学声子解析表达式的拟合方法除虚晶近似(VCA)外, 还有简化相干势近似(SCPA)^[8]、忽略统计相关性的无规元素等位移模型(MREI)^[9]等. 然而, 这几种方法均属单模近似, 未能

引用格式: 屈媛, 宗易昕, 马健, 等. 体横光学声子双模性对纤锌矿 $\text{Al}_x\text{Ga}_{1-x}\text{N}$ 量子阱中光学声子的影响. 中国科学: 物理学 力学 天文学, 2014, 44: 150-161
Qu Y, Zong Y X, Ma J, et al. Optical phonons in wurtzite $\text{Al}_x\text{Ga}_{1-x}\text{N}$ quantum wells affected by two-mode property of TO phonons (in Chinese). Sci Sin-Phys Mech Astron, 2014, 44: 150-161, doi: 10.1360/132013-161

Spin-polarized transport through ZnMnSe/ZnSe/ZnBeSe heterostructures

Y. Ming,¹ J. Gong,^{1,a)} and R. Q. Zhang²¹*School of Physics Science and Technology, Inner Mongolia University, Hohhot 010021, People's Republic of China*²*Department of Physics and Materials Science, City University of Hong Kong, Tat Chee Avenue, Hong Kong, People's Republic of China*

(Received 22 June 2011; accepted 5 October 2011; published online 9 November 2011)

Using the transfer matrix method and Airy function, the spin-dependent tunneling through the ZnMnSe/ZnSe/ZnBeSe structure was investigated theoretically. The electron tunneling determined by the applied bias, external magnetic field, and spin orientations exhibited some interesting and complex features. It was found that the magnetic field could suppress the spin-up current, but enhance the spin-down current. Furthermore the spin-flip of current could be realized by changing the applied bias slightly. Therefore, it can be believed that our structure could behave as a good spin-filter. © 2011 American Institute of Physics. [doi:10.1063/1.3658852]

I. INTRODUCTION

In recent years, the interdisciplinary field called “spintronics” has attracted increasing attention.^{1–5} A number of experiments have shown that the spin of electrons has a relative large phase-coherent length of up to 0.1 mm and a surprising long dephasing time of several microseconds.^{6,7} Consequently, many novel applications have been proposed, such as spin-FET (field effect transistor), spin-LED (light-emitting diode), spin-RTD (resonant tunneling devices), encoders, decoders, and quantum bits. However, many problems such as electrical spin injection, optical manipulation, spin coherence, etc. remain to be worked out before the realizing of spintronics devices. In recent years, spin injection and spin filter effect have been studied in semiconductor quantum dot systems.^{8–10} For these problems, spin injection with high efficiency and high polarization rate is a crucial subject. Due to the mismatch of crystal constant, spin injections from metal to semiconductor usually have a low efficiency. A typical example is spin injection from Fe to GaAs with efficiency of 2%, which was observed by Zhu *et al.*⁵

The diluted magnetic semiconductors (DMSs) have been proposed in order to overcome the obstacle above.¹¹ Since then, more and more heterostructures and quantum wells consisting of the III–V DMSs have attracted a great deal of research interests.^{12,13} Tanaka *et al.* have investigated the spin-dependent tunneling properties in the GaMnAs quantum-well double-barrier heterostructures.^{14–16} They have clearly observed the resonant tunneling effect and the increase of tunnel magnetoresistance (TMR) induced by resonant tunneling.¹⁴ Recently, they successfully controlled the quantum levels and modulated the spin-dependent current with varying the voltage of the electrode connected to the GaMnAs QW.¹⁵ However, the II–VI DMSs have the similar conductivity comparable to that of typical nonmagnetic semiconductors (NMSs) and can be *n*-type doped so that the fast spin precession could be avoided.¹⁷ Besides, they are promising for applications in the construction of photo- and

electrooptical devices operating in blue–green and ultraviolet spectral regions. As a result, II–VI DMSs are known to be better candidates for effective spin injection into a NMS.

Slobodskyy *et al.* have investigated the current–voltage characteristics of an II–VI semiconductor resonant tunneling diode coupled to a diluted magnetic semiconductor injector.⁴ The negative differential conductance has been observed. However, the spin polarization rate was not discussed in their paper.

The effects of Mn concentration on spin-polarized current density through ZnSe/ZnMnSe/ZnSe heterostructures have also been investigated by Saffarzadeh *et al.*¹⁸ It has been found that spin polarization rate on the whole would rise with the increase of Mn concentration. Unfortunately, the influence of magnetic field on the polarization rate was not investigated in their work. The Fermi energy as an important parameter determines the incident energy of the electron. The effect of Fermi energy on the polarization rate was also not discussed in their calculation.

In this paper, we analyze the spin-dependent tunneling through a multilayer structure consisting of ZnMnSe, ZnSe, and ZnBeSe. It is found that negative conductance appeared in the *J*–*V* curve. The spin polarization rate as high as 95% is observed; and the spin orientation can be tuned by the adjustment of applied bias.

II. THEORETICAL MODEL

We consider the ballistic transport of a conduction electron traversing a band-gap-matched ZnSe/ZnMnSe/ZnSe/ZnBeSe/ZnSe/ZnBeSe/ZnSe heterostructure. (See Fig. 1) L_2 is the width of ZnMnSe layer, and L_4 , L_6 are the widths of two ZnBeSe layers, respectively. The three layers mentioned above are separated by two ZnSe layers with widths of L_3 and L_5 .

In order to enhance the coupling between two $Zn_{1-y}Be_ySe$ layers, the Be concentration y and the widths of them are assumed to be identical, respectively ($y = 0.008$, $L_4 = L_6 = 10$ nm). As a result, the conduction offset under the zero magnetic field can be written as:

^{a)}Electronic mail: ndgong@imu.edu.cn.

Quasi-Classical Trajectory Stereodynamics Study of the Li + HF($v = 0, j = 0$) \rightarrow LiF + H Reaction

MING-HU YUAN, GUO-JUN ZHAO

Department of Physics, School of Physical Science and Technology, Inner Mongolia University, Hohhot 010021, People's Republic of China

Received 25 March 2009; accepted 26 May 2009

Published online 3 November 2009 in Wiley InterScience (www.interscience.wiley.com).

DOI 10.1002/qua.22374

ABSTRACT: In this work, quasi-classical trajectory (QCT) calculations for the Li + HF ($v = 0, j = 0$) \rightarrow LiF + H reaction, on the Aguado-Paniagua2-potential energy surface (AP2-PES) constructed by Aguado et al. (Aguado et al., *J Chem Phys* 1997, 107, 10085), have been performed to study the vector properties of the products. The dihedral angle distribution $P(\phi_r)$ characterizing the k-k'-j' correlation and the $P(\theta_r)$ distribution characterizing the k-j' correlation are calculated and discussed. Furthermore, the angular distribution $P(\theta_r, \phi_r)$ of product rotational vectors plotted in polar form in θ_r and ϕ_r is presented. Finally, the average rotational alignment factor $\langle P_2(\cos\theta_r) \rangle$ is calculated over a collision energy range of 20–450 meV to investigate the variation of the rotational alignment with collision energy. © 2009 Wiley Periodicals, Inc. *Int J Quantum Chem* 110: 1842–1847, 2010

Key words: quasi-classical trajectory; rotational alignment; stereodynamics

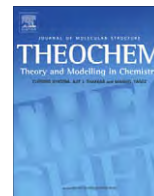
1. Introduction

In the last thirty years, a great deal of experimental [1–4] and theoretical [5–15] work has been devoted to the Li + HF reaction, a prototype of the heavy-heavy-light (HHL) system and a benchmark in molecular reaction dynamics. The reaction is known to have a strongly bent transition state, and this feature is expected to add a considerable richness to its dynamics [6].

Correspondence to: G. Zhao; e-mail: stzhaogj@imu.edu.cn

A number of experiments have been carried out to explore the underlying reaction mechanism of the title reaction. In a crossed molecular beam study by Becker et al. [1], mass spectrometry was used to detect the LiF product and its angular distribution in the laboratory frame; in addition, time-of-flight spectra were measured at several collision energies. Afterward, Loesch et al. [2–4] reported the detailed crossed molecular beam studies on the Li + HF($v = 1, j = 1, m = 0$) reaction at the collision energy $E_{\text{coll}} = 420$ meV.

At the same time, the title reaction is attractive for theoretical treatments due to its relative simplic-



Application of the sixth-order symplectic integration to the chemical stereodynamics for the reactions $\text{Li} + \text{H}(\text{D})\text{F} (v = 0, j = 0) \rightarrow \text{LiF} + \text{H}(\text{D})$

Ming-Hu Yuan, Guo-Jun Zhao*

Department of Physics, School of Physical Science and Technology, Inner Mongolia University, Hohhot 010021, China

ARTICLE INFO

Article history:

Received 22 July 2009

Received in revised form 1 September 2009

Accepted 1 September 2009

Available online 4 September 2009

Keywords:

Quasi-classical trajectory

Sixth-order symplectic integration

Dynamical stereochemistry

ABSTRACT

Studies on the dynamical stereochemistry of the $\text{Li} + \text{HF}$ reaction and its isotopic variants have been performed using quasi-classical trajectory (QCT) method with the sixth-order symplectic integration on the AP2-PES which is produced by Aguado et al. [A. Aguado, M. Paniagua, M. Lara, O. Roncero, J. Chem. Phys. 107 (1997) 10085]. The polarization-dependent differential cross-sections (PDDCSs) have been calculated and compared. In addition, comparisons of the distributions $P(\theta_r)$, $P(\phi_r)$ and of the average rotational alignment factor $\langle P_2(\cos \theta_r) \rangle$ are given for the isotopic variants.

© 2009 Elsevier B.V. All rights reserved.

1. Introduction

In the last 30 years, a great deal of experimental [1–4] and theoretical [5–15] work has been devoted to the $\text{Li} + \text{HF}$ reaction, a prototype of the heavy–heavy–light (HHL) system and a benchmark in molecular reaction dynamics. The reaction is known to have a strongly bent transition state, and this feature is expected to add a considerable richness to its dynamics.

Lots of experiments have been carried out to explore the underlying reaction mechanism of the title reaction. In a crossed molecular beam study of Becker et al. [1], mass spectrometry was used to detect the LiF product, and the product laboratory angular distributions as well as the time-of-flight spectra were measured at several collision energies. Afterwards, Loesch and coworkers [2–4] reported the detailed crossed molecular beam studies on the $\text{Li} + \text{HF} (v = 1, j = 1, m = 0)$ reaction.

At the same time, the title reaction is attractive for theoretical treatments because of its relative simplicity. It is important to make an ideal potential energy surface (PES) for carrying out the theoretical studies. And there exists a series of semi-empirical and *ab initio* potential energy surface and a variety of dynamical calculations. Aguado et al. [13] have carried out wave packet calculations on their original PES and found a substantially lower reactivity than on the Laganà PES [14]. Subsequently, a new refined version of the original PES, fitted using more *ab initio* energy points, has been produced and reported by the same authors [15] (hereafter named AP2-PES). This new fit lowered the saddle-point

energy to 0.233 eV and suppressed the spurious features of the initial fit.

Based on the AP2-PES, we studied the stereodynamics features of the reactions using quasi-classical trajectory (QCT) method with the sixth-order symplectic integration. From a previous paper [16], it is found that the symplectic integration can be employed as a replacement of traditional integrators as the “method of choice” for stable, inexpensive performance, e.g., it is six times faster with an excellent accuracy of energy conservation for the $\text{O}(\text{D}) + \text{H}_2$ reaction.

Isotope effect on the stereodynamics is significant for many reactions [17,18], while vector properties are important for studying the stereodynamics underlying a chemical reaction. And many experimental techniques, such as the polarization-resolved chemiluminescence [19,20], the polarized laser-induced fluorescence [21,22], the electric deflection methods [23,24], can be used under molecular beam [25] and bulb conditions to determine the product vector properties. Meanwhile, there are many important theoretical works describing classical and quantum treatments of stereodynamics in chemical reactions [26,27,5,28]. In this work, in order to investigate the mass effect on the underlying stereodynamics, we calculated the PDDCSs and the average rotational alignment factor $\langle P_2(\cos \theta_r) \rangle$ for both the $\text{Li} + \text{HF}$ and $\text{Li} + \text{DF}$ reactions by using the QCT method. As is well known, the most important vector correlation is the correlation among the three vectors \mathbf{k} , \mathbf{k}' (the reagent and product relative velocities) and \mathbf{j}' (the product rotational angular momentum). Hence, in this paper, we employed the sixth-order symplectic integration to calculate $P(\theta_r)$ and $P(\phi_r)$ for the two reactions, with $P(\theta_r)$ and $P(\phi_r)$ being the angular distributions characterizing the $\mathbf{k}\text{--}\mathbf{j}'$ and $\mathbf{k}\text{--}\mathbf{k}'\text{--}\mathbf{j}'$ correlations.

* Corresponding author.

E-mail address: stzhaogj@imu.edu.cn (G.-J. Zhao).